Finite Formulation of Surface Impedance Boundary Conditions

Finite Formulation of Surface Impedance Boundary Conditions

Vincenzo Cirimele[1], Fabio Freschi[1,2], Luca Giaccone[1], and Maurizio Repetto[1,2]

[1]Department of Energy, Politecnico di Torino, Turin 10129, Italy
[2]School of Information Technology and Electrical Engineering, The University of Queensland, St Lucia, QLD 4072, Australia

In several electromagnetic applications, field quantities are confined in layers that are thin with respect to other geometrical dimensions. The numerical solution of these phenomena has led to the development of special formulations. Among these, the surface impedance boundary conditions (SIBCs) have been extensively investigated in the past decades, often coupling them to other techniques for the analysis of volumes, such as the finite-element or boundary element methods. In this paper, the SIBCs are presented by the light of finite formulation and extended to include the considered magnetic nonlinearity.

***Index Terms*— Boundary element method (BEM), finite formulation, hybrid techniques, surface impedance boundary condition (SIBC).**

I. Introduction

THE ANALYSIS of physical problems has often to handle different geometrical scales and sub-domains with dimensions that are much smaller than the overall ones. The brute force application of a volume-based numerical analysis can lead to inaccurate and unaffordable results. The use of hybrid numerical techniques, coupling together volume-based methods with the particular treatment of the smaller sub-domain, has shown to be an efficient, even if non standard, approach and related to the particular problem under study.

Among these techniques, the use of the surface impedance boundary conditions (SIBCs) is a technique, which can be used to treat electromagnetic phenomena in time-varying electromagnetics. Many works have discussed the main aspects of the SIBC both from the theoretical and implementation viewpoints, such as in [1]–[3]. The use of the SIBC is generally limited to a linear magnetic material. An attempt to extend the method to nonlinear magnetic materials is the subregion sequence approach proposed in [4]–[6].

The main difficulty in dealing with nonlinear materials is related to the strict dependence of the skin effect on the effective material permeability, which is changing very rapidly due to the boosting of the magnetic flux density close to the surface [7].

This work develops a formalism based on the primal/dual discretization of the surface, ideally linked to the concepts of the cell method developed in [8] and [9], that naturally leads to a circuit representation of the eddy-current phenomenon, and couples this formulation with the boundary element method (BEM). Nonlinearity is, thus, treated not in terms of local quantities, like magnetic permeability values, but directly in terms of the resulting nonlinear surface impedance, which is computed offline by means of the solution of a 1-D problem.

II. Nonlinear SIBC Formulation

The considered domain is made by a magnetic and conductive simply connected volume surrounded by space where sources, conductors with impressed currents, are present. It is considered that the external region is studied by means of the BEM formulated in terms of reduced scalar magnetic potential. It is assumed that the penetration depth of the electromagnetic quantities is much smaller than the other geometrical dimensions so that the volume is replaced by its boundary surface. The electromagnetic phenomena inside the conductive region are depending only on the depth coordinate y. A sketch of the local coordinate on the surface of the conductive domain and of the main field quantities is shown in Fig. 1.

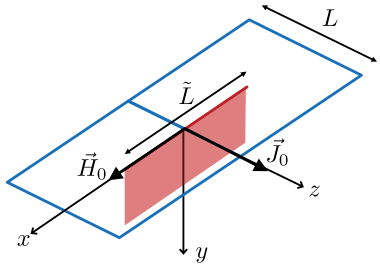

Fig. 1. Local coordinate system on the surface of the conductive domain. The y coordinate is along the depth.

A. Circuit Formulation of Eddy Currents

The boundary of the volume is discretized with two intertwined grids linked by duality relation, as shown in Fig. 2. Instead of formulating the problems in terms of local quantities, such as current densities and electric field, global variables are used, i.e., quantities associated with space entities.

Concerning the current formulation, electromotive forces e are defined on primal edges, and magnetic fluxes ϕ are defined on primal faces. Magnetomotive forces h and currents i are defined, respectively, on dual edges and faces. The depth of the dual face extends through the depth until the value where all the field quantities vanish. Magnetomotive forces, in turn, can be expressed as the gradient of the magnetic scalar potential ψ defined on dual nodes. When considering a sinusoidal time-harmonic formulation, the phasor quantities can be used.

The topological equations of the electromagnetic fields can be written directly in terms of global variables. The discrete version of Faraday's law in a matrix form is

$$\mathbf{Ce} = -\mathrm{j}\omega\boldsymbol{\phi} \tag{1}$$

Manuscript received July 6, 2015; revised September 4, 2015; accepted October 5, 2015. Date of publication October 14, 2015; date of current version February 17, 2016. Corresponding author: M. Repetto (e-mail: maurizio.repetto@polito.it).

Color versions of one or more of the figures in this paper are available online at http://ieeexplore.ieee.org.

Digital Object Identifier 10.1109/TMAG.2015.2490102

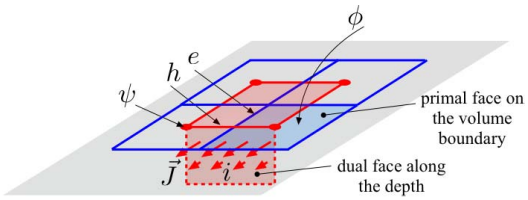

Fig. 2. Dual discretization of the conductive domain by considering the depth coordinate. Blue lines: primal grid. Red lines: dual grid.

where $\mathbf{C}$ is the primal face-edge incidence matrix [8], $\mathbf{e}$ is the vector of electromotive forces along primal edges, $\boldsymbol{\phi}$ is the vector of magnetic fluxes through primal faces, and ω is the angular frequency. Ampère's law becomes

$$\mathbf{h} = \mathbf{i} \tag{2}$$

where $\mathbf{h}$ is the vector of magnetomotive forces along dual edges and $\mathbf{i}$ is the vector of currents through the dual faces defined in Fig. 2. This expression comes from the fact that, of the four edges bounding the dual face, only the one lying on the conductor surface leads to a non-null contribute to the circulation of the magnetic field. On the opposite edge, the field is null, because the face is extending to the depth where all the field quantities disappear and the other two edges are orthogonal to the magnetic field direction. By considering a linear conductive material characterized by the magnetic permeability μ and the electrical conductivity σ, the constitutive equation tying together the surface electric field and the surface value of the current density can be written as

$$i = \int_{\tilde{L}} \int_0^{+\infty} J_0 e^{-\frac{y}{\delta}} e^{-j\frac{y}{\delta}} dy dL = \tilde{L} \frac{\delta}{1+j} \frac{\sigma e}{L} = Ye \tag{3}$$

where Y is the admittance linking e to the current i, L and $\tilde{L}$ are the length of the primal and dual edges (Fig. 1), and δ is the penetration depth, defined as $\delta = (2/\omega\mu\sigma)^{1/2}$. The circuit relation can also be written as $e = Y^{-1}i = Zi$, where Z is the impedance of the circuit element represented by the primal edge-dual face couple. The impedances of all the primal edge-dual face couples are collected in the diagonal matrix $\mathbf{Z}$.

The relation defined in (3) links each electromotive force on primal edge to the current flowing through the corresponding dual face. Using Faraday's law (1), a circuit representation can be introduced as

$$\mathbf{Ce} = -\mathrm{j}\omega\boldsymbol{\phi} \Rightarrow \mathbf{CZi} = -\mathrm{j}\omega\boldsymbol{\phi}. \tag{4}$$

Using the mesh current $\mathbf{i}_{\mathrm{mesh}}$ [10], (4) can be written as

$$\mathbf{i} = \mathbf{C}^T\mathbf{i}_{\mathrm{mesh}} \Rightarrow \mathbf{CZC}^T\mathbf{i}_{\mathrm{mesh}} = -\mathrm{j}\omega\boldsymbol{\phi}. \tag{5}$$

The system in (5) has a number of equations equal to the number of primal faces on the domain surface, and can be solved once the incident magnetic fluxes $\boldsymbol{\phi}$ are known.

B. Nonlinear Eddy Currents

When the material magnetic characteristic is nonlinear, the admittance, defined in (3), cannot be expressed in closed form. Nonlinear effects are treated by means of an equivalent material that, under a sinusoidal excitation, gives the same response of the actual nonlinear material in terms of coenergy [11].

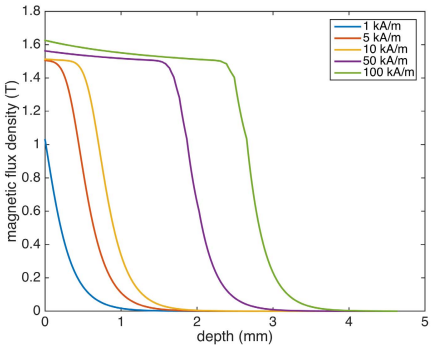

Fig. 3. Magnetic flux density along the depth of a material with the nonlinear characteristic defined in (10) for different values of the surface magnetic field with $B_s = 1.5$ T and $\mu_r = 1000$.

This approach substitutes to the nonlinear ferromagnetic material an equivalent $B(H)$ characteristic, based on a coenergy equivalence, and has been efficiently applied to induction heating problems, as, for instance, in [12]. The working point on the characteristic depends on the peak value of the magnetic flux density sine wave and not on its instantaneous value.

The 1-D diffusion equations in the frequency domain is expressed as

$$\frac{\partial^2 H}{\partial y^2} = j\omega\sigma\,(\mu_{\mathrm{FP}}H + R) \tag{6}$$

$$H(y=0) = H_0 \tag{7}$$

$$H(y\to\infty) = 0. \tag{8}$$

Equation (6) is numerically discretized by the 1-D finite-difference method, while the magnetic nonlinearity is solved by means of the fixed point technique as

$$B = \mu_{\mathrm{FP}}H + R \tag{9}$$

where μ_{FP} is a constant permeability value and R is the nonlinear residual that has to be updated iteratively [13]. The solution of (6) gives the behavior of the field penetration inside the material.

Using a simplified nonlinear characteristic expressed as

$$B = B_s \tanh\left(\frac{\mu_r\mu_0 H}{B_s}\right) + \mu_0 H \tag{10}$$

where the two parameters B_s and μ_r characterize the nonlinear curve, and the pattern of the magnetic flux density along the depth can be drawn for different values of the surface magnetic field H_0. The values in Fig. 3 are computed by considering $B_{\mathrm{s}} = 1.5$ T, $\mu_{\mathrm{r}} = 1000$, electrical conductivity $\sigma = 5.8$ MS/m, and frequency $f = 1$ kHz, leading to a value of penetration depth $\delta = 0.21$ mm in the linear zone.

The corresponding solution for the current density is obtained by the numerical differentiation of the solution of (6)

$$J(y) = -\frac{dH}{dy} = -\frac{\Delta H}{\Delta y}. \tag{11}$$

The penetration of the field quantities increases together with the saturation level, giving rise to a nonlinear increase in the current flowing through the depth. This phenomenon is

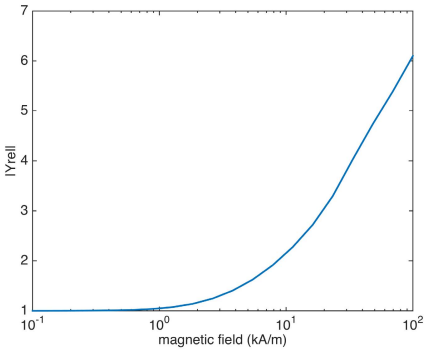

Fig. 4. Variation of the parameter $|Y_{\text{rel}}|$ as a function of the applied magnetic field.

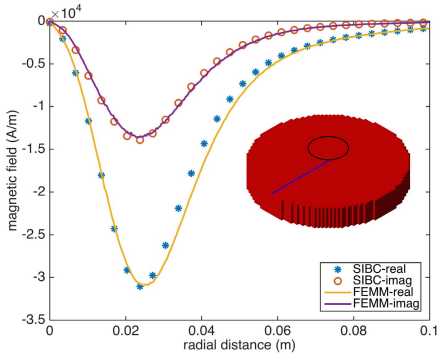

Fig. 5. Tangential component of the magnetic field on the disk surface: 2-D axisymmetric (FEMM) and SIBC-BEM at 10 kHz.

well appreciable by looking at the behavior of the admittance as a function of the applied surface magnetic field H_0 as

$$Y(H_0) = \frac{i}{e} = \frac{\sigma \tilde{L}}{L J_0(H_0)} \int_0^{+\infty} J(y)dy. \tag{12}$$

The resulting effect of the admittance can be seen in Fig. 4, where the value of the admittance normalized with respect to its value in the linear zone is shown $|Y_{\text{rel}}| = |Y(H_0)/Y_{\text{linear}}|$. The nonlinear behavior of the admittance is changing with the applied magnetic field, but its nonlinearity does not show abrupt changes in slope, since the saturation effect, well visible in the B values (Fig. 3), is smoothed out by the increase in the penetration depth. The characteristic of $Y(H_0)$ is tabulated for each nonlinear material and interrogated at each nonlinear iteration.

III. Hybrid SIBC-BEM Formulation

The lumped parameters formulation of the eddy currents inside the material is coupled to the BEM technique for the analysis of the external domain where source conductors with impressed currents are considered. The BEM problem is formulated in terms of the reduced magnetic scalar potential ψ. The magnetic field in the external region is given by

$$\vec{H} = -\nabla\psi + \vec{H}_S \tag{13}$$

where $\vec{H}_S$ is the magnetic field created by imposed current sources. When the source currents are sinusoidal in time, all the previous quantities can be expressed by phasors. The BEM equations are then given by

$$\mathbf{H}\boldsymbol{\psi} + \mathbf{W}\frac{\partial \boldsymbol{\psi}}{\partial \mathbf{n}} = 0 \tag{14}$$

where matrices $\mathbf{H}$ and $\mathbf{W}$ are derived by the standard formulation as in [14]. The two formulations are coupled by means of the physical continuity of field at the conductor surface.

By imposing the continuity of the normal component of the magnetic flux density at the interface, the normal derivative of the magnetic scalar potential can be linked to the incident magnetic flux present in (4) by

$$\boldsymbol{\phi} = \mu_0 \mathbf{A}\left(-\frac{\partial \boldsymbol{\psi}}{\partial \mathbf{n}} + \mathbf{H}_{Sn}\right) \tag{15}$$

where $\mathbf{A}$ is a diagonal matrix, containing the area of each primal face. As a consequence, the circuit equation can be reformulated as

$$\mathbf{C}\mathbf{Z}\mathbf{C}^T\mathbf{i}_{\text{mesh}} = -\mathbf{S}\left(\frac{\partial \boldsymbol{\psi}}{\partial \mathbf{n}} - \mathbf{H}_{Sn}\right) \tag{16}$$

where $\mathbf{S} = j\omega\mu_0\mathbf{A}$. By exploiting Ampère's law of (2), the tangential component of the magnetic field is

$$\mathbf{i} = \mathbf{C}^T\mathbf{i}_{\text{mesh}} = -\mathbf{C}^T\boldsymbol{\psi} + \mathbf{h}_S. \tag{17}$$

By coupling together the BEM and the circuit equations, the hybrid formulation can be obtained as

$$\begin{bmatrix} \mathbf{H} & \mathbf{W} \\ -\mathbf{C}\mathbf{Z}\mathbf{C}^T & \mathbf{S} \end{bmatrix} \begin{bmatrix} \boldsymbol{\psi} \\ \dfrac{\partial \boldsymbol{\psi}}{\partial \mathbf{n}} \end{bmatrix} = \begin{bmatrix} \mathbf{0} \\ \mathbf{S}\mathbf{H}_{Sn} - \mathbf{C}\mathbf{Z}\mathbf{h}_S \end{bmatrix} \tag{18}$$

where impedance matrix $\mathbf{Z}$ can be nonlinear as described in Section II-B.

The lower right block $\mathbf{S}$ of the coefficient matrix is diagonal, and this characteristic can be exploited by calculating the Schur complement of $\mathbf{S}$ and solving with respect to $\partial\boldsymbol{\psi}/\partial\mathbf{n}$

$$\frac{\partial \boldsymbol{\psi}}{\partial \mathbf{n}} = -\mathbf{H}_{Sn} + \mathbf{S}^{-1}(\mathbf{C}\mathbf{Z}\mathbf{C}^T\boldsymbol{\psi} - \mathbf{C}\mathbf{Z}\mathbf{h}_S) \tag{19}$$

then, substituting (19) in (18)

$$(\mathbf{H} + \mathbf{W}\mathbf{S}^{-1}\mathbf{C}\mathbf{Z}\mathbf{C}^T)\boldsymbol{\psi} = \mathbf{W}(\mathbf{H}_{Sn} + \mathbf{S}^{-1}\mathbf{C}\mathbf{Z}\mathbf{h}_S). \tag{20}$$

The system is solved using GMRES, avoiding the effective assembling of $\mathbf{H} + \mathbf{W}\mathbf{S}^{-1}\mathbf{C}\mathbf{Z}\mathbf{C}^T$ but supplying the solver with the matrix–vector product $\mathbf{H}\boldsymbol{\psi} + \mathbf{W}\mathbf{S}^{-1}\mathbf{C}\mathbf{Z}\mathbf{C}^T\boldsymbol{\psi}$. Due to the smooth nonlinear Y characteristic, a simple nonlinear scheme, where the value of $Y(H_0)$ is iteratively updated, is adopted to solve (20) with nonlinear materials.

IV. Results and Discussion

The proposed numerical scheme has been validated by solving a nonlinear eddy-current problem in a cylindrical conductive domain of radius 10 cm and thickness 3 cm with electric and magnetic properties used to obtain the results in Fig. 3. The source is a filamentary circular conductor having a radius of 2.5 cm placed at a distance of 2 cm above the conducting disk with a sinusoidal current of 5 kA. The results are compared with a 2-D axisymmetric solution [15]. Fig. 5 compares the tangential component of the magnetic field on the disk surface at 10 kHz when the material is saturated

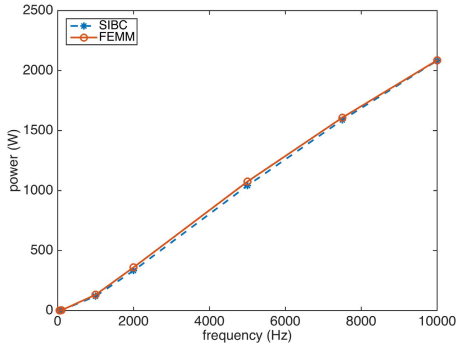

Fig. 6. Variation of the losses inside the conductive domain as a function of supplying frequency.

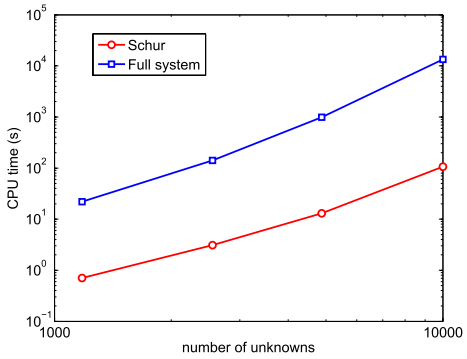

Fig. 7. CPU times of different approaches to the solution of (18).

(compare the values of the magnetic field with the curves shown in Fig. 3). The power losses at different saturation levels, obtained ranging the frequency from 50 to 10 kHz, are represented in Fig. 6. The two methods are in good agreement when comparing local and global quantities. The nonlinear scheme always converged in less than 25 iterations for a maximum value of the applied magnetic field of ∼30 kA. The benefits of the Schur complement technique are assessed by looking at the solution time for two GMRES solutions: 1) considering the original scheme (18) and 2) using (20). As shown in Fig. 7, the advantage of using the Schur complement is to always reduce the computational cost of more than one order of magnitude. The technique implemented has shown good convergence capabilities and accurate results. This work will continue in extending the technique to unstructured surface meshes.

REFERENCES

[1] B. Ancelle, A. Nicolas, and J. C. Sabonnadière, "A boundary integral equation method for high frequency eddy currents," *IEEE Trans. Magn.*, vol. 17, no. 6, pp. 2568–2570, Nov. 1981.

[2] L. Krähenbühl and D. Muller, "Thin layers in electrical engineering-example of shell models in analysing eddy-currents by boundary and finite element methods," *IEEE Trans. Magn.*, vol. 29, no. 2, pp. 1450–1455, Mar. 1993.

[3] I. D. Mayergoyz and G. Bedrosian, "On calculation of 3-D eddy currents in conducting and magnetic shells," *IEEE Trans. Magn.*, vol. 31, no. 3, pp. 1319–1324, May 1995.

[4] B. Paya and C. Guérin, "Magnetic field dependence of nonlinear surface impedance: Which field to choose?" *IEEE Trans. Magn.*, vol. 38, no. 2, pp. 585–588, Mar. 2002.

[5] K. Ishibashi, Z. Andjelic, and D. Pusch, "Nonlinear eddy current analysis by bem utilizing adaptive equation technique," *IEEE Trans. Magn.*, vol. 45, no. 3, pp. 1020–1023, Mar. 2009.

[6] K. Ishibashi, Z. Andjelic, and D. Pusch, "Nonlinear eddy current analysis by boundary integral equation of one component utilizing impedance boundary condition," *IEEE Trans. Magn.*, vol. 47, no. 5, pp. 1398–1401, May 2011.

[7] A. Canova *et al.*, "Simplified approach for 3-D nonlinear induction heating problems," *IEEE Trans. Magn.*, vol. 45, no. 3, pp. 1855–1858, Mar. 2009.

[8] E. Tonti, "Finite formulation of electromagnetic field," *IEEE Trans. Magn.*, vol. 38, no. 2, pp. 333–336, Mar. 2002.

[9] P. Alotto, F. Freschi, and M. Repetto, "Multiphysics problems via the cell method: The role of Tonti diagrams," *IEEE Trans. Magn.*, vol. 46, no. 8, pp. 2959–2962, Aug. 2010.

[10] C. A. Desoer and E. S. Kuh, *Basic Circuit Theory*. New York, NY, USA: McGraw-Hill, 1969.

[11] A. Kost, J. P. A. Bastos, K. Miethner, and L. Jänicke, "Improvement of nonlinear impedance boundary conditions," *IEEE Trans. Magn.*, vol. 38, no. 2, pp. 573–576, Mar. 2002.

[12] F. Freschi, L. Giaccone, and M. Repetto, "Magneto-thermal analysis of induction heating processes," *Comput. Model. Eng. Sci.*, vol. 94, no. 5, pp. 371–395, 2013.

[13] M. Chiampi, D. Chiarabaglio, and M. Repetto, "An accurate investigation on numerical methods for nonlinear magnetic field problems," *J. Magn. Magn. Mater.*, vol. 133, pp. 591–595, May 1994.

[14] W. M. Rucker and K. R. Richter, "Three-dimensional magnetostatic field calculation using boundary element method," *IEEE Trans. Magn.*, vol. 24, no. 1, pp. 23–26, Jan. 1988.

[15] D. Meeker. *Finite Element Method Magnetics, Version 4.2*. [Online]. Available: http://www.femm.info, accessed Oct. 10, 2015.